MAYO CLINIC

ORIGINAL ARTICLE

Combining Shape-Sensing Robotic Bronchoscopy With Mobile Three-Dimensional Imaging to Verify Tool-in-Lesion and Overcome Divergence: A Pilot Study

Janani Reisenauer, MD; Jennifer D. Duke, MD; Ryan Kern, MD; Sebastian Fernandez-Bussy, MD; and Eric Edell, MD

Abstract

Objective: To determine whether CT-to-body divergence can be overcome to improve the diagnostic yield of peripheral pulmonary nodules with the combination of shape-sensing robotic-assisted bronchoscopy (SSRAB) and portable 3-dimensional (3D) imaging.

Patients and Methods: A single-center, prospective, pilot study was conducted from February 9, 2021, to August 4, 2021, to evaluate the combined use of SSRAB and portable 3D imaging to visualize tool-in-lesion as a correlate to diagnostic yield.

Results: Thirty lesions were subjected to biopsy in 17 men (56.7%) and 13 women (43.3%). The median lesion size was 17.5 mm (range, 10-30 mm), with the median airway generation of 7 and the median distance from pleura of 14.9 mm. Most lesions were in the upper lobes (18, 60.0%). Tool-in-lesion was visualized at the time of the procedure in 29 lesions (96.7%). On the basis of histopathologic review, 22 (73.3%) nodules were malignant and 6 (20.0%) were benign. Two (6.7%) specimens were suggestive of inflammation, and the patients elected observation. The mean number of spins was 2.5 (±1.6) with a mean fluoroscopy time of 8.7 min and a mean dose area product of 50.3 Gy cm^2 (±32.0 Gy cm^2). There were no episodes of bleeding or pneumothorax. The diagnostic yield was 93.3%.

Conclusion: This pilot study shows that the combination of mobile 3D imaging and SSRAB of pulmonary nodules appears to be safe and feasible. In conjunction with appropriate anesthetic pathways, nodule motion and divergence can be overcome in most patients.

Trial Registration: https://clinicaltrials.gov Identifier NCT04740047

 ■ Mayo Clin Proc Inn Qual Out 2022;6(3):177-185

Lung cancer is the leading cause of cancer-related mortality in men and women throughout the world.[1,2] In 2019, primary bronchogenic cancers accounted for 23% of all cancer deaths in the United States.[3] Besides the aggressive nature of the disease, the overall high mortality is related to the delay between the emergence of the first cancer cells and the time to diagnosis.[4,5] Overall, the 5-year survival is only 21.7% (2011-2017), whereas the relative survival for lung cancer confined to the primary side can be as high as 59.8%.[6] The 5-year survival of patients with metastatic cancer at diagnosis is only 6.3%.[6] To detect lung cancer at an earlier stage, annual screening for at-risk individuals is recommended, which has led to an increased detection of pulmonary nodules.[7]

Historically, bronchoscopy has played only a limited role in pulmonary nodule management because of the limited diagnostic accuracy of 14%-31%.[8] Percutaneous nodule biopsy has a pneumothorax rate of 12-45%.[9] Newer bronchoscopic techniques include radial endobronchial ultrasound (rEBUS), electromagnetic navigation bronchoscopy

From the Division of Thoracic Surgery (J.R.), and Division of Pulmonary and Critical Care Medicine (J.R., J.D.D., R.K., E.E.), Mayo Clinic Rochester MN; and Division of Pulmonary and Critical Care Medicine (S.F.-B.), Mayo Clinic, Jacksonville, FL.

(ENB), virtual bronchoscopic navigation, and more recently, robotic-assisted bronchoscopy that has increased the diagnostic yield.[10] However, data suggest that the diagnostic yield may be associated with a patent proximal bronchus.[11] With the emergence of robotic bronchoscopy, proceduralists can now navigate farther in the airways to lesions completely extrinsic to the airways, with biopsy yields reported from 69.1%-81.7%.[12-15]

Despite the increased diagnostic yield from robotic-assisted bronchoscopy, challenges in the exact localization of the lesion can be due to changes in lung anatomy in a mechanically ventilated patient when compared with the preprocedural computed tomography (CT) scan-derived anatomy obtained from a spontaneously breathing patient relied upon for navigation. This phenomenon is termed "CT-to-body divergence" and represents a challenge to the proceduralist.[16] Slight changes in positioning from diaphragmatic movement can distort the nodule position, alter the "virtual target," and impact the diagnostic and procedural outcomes.

Cone-beam computed tomography (CBCT) on fixed C-arms has been used to complement the localization of nodules by producing CT-like cross-sectional multiplanar and 3-dimensional (3D) images.[17] As CBCT is performed during the procedure, the image captured during the spin should have minimal body divergence. Studies using CBCT have shown better targeting accuracy and low radiation dose using this technology.[18,19] Recently, the combination of CBCT with electromagnetic navigation was shown to increase the diagnostic accuracy from 72%-90% with a procedural radiation exposure as measured by the dose area product (DAP) initially of 47.5 Gy cm^2, which was gradually brought down to 25.4 Gy cm^2 with increasing experience and by tailoring the imaging protocols.[20,21]

The advent of portable 3D fluoroscopy systems can overcome these hurdles. The CIOS 3D Spin Mobile (Siemens Healthineers) is a compact C-arm (Figure 1) that is electronically rotated around the patient's chest by ±100° to generate a CT image and confirm the tool-in-lesion before sampling.[17] The base of the 3D mobile imaging system sits laterally to the patient's chest and leaves the head clear for equipment and personnel. The images generated with the mobile 3D imaging system may be of lower quality compared with those from fixed CBCT imaging, and the time needed for image acquisition is longer (30 s for CIOS vs 5.2 s for the Philips Azurion system).

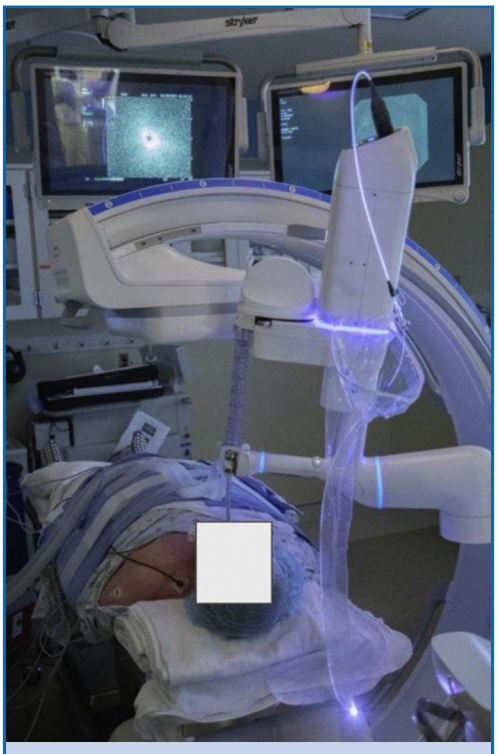

FIGURE 1. CIOS system seen at the patient's right side with positioning allowing for the robotic bronchoscopic platform to be situated at the patient's head.

PATIENTS AND METHODS

Study Cohort

This was a prospective, single-center, single-arm pilot study to evaluate the clinical utility and early performance of the CIOS 3D Mobile Spin system in conjunction with the Ion Endoluminal System to visualize and facilitate the sampling of peripheral pulmonary nodules between 1 and 3 cm (NCT04740047). After approval by the Mayo Clinic institutional review board (IRB#20-004757), 32 patients provided written consent and were enrolled between February 9, 2021, and August 4, 2021. Consecutive patients who met the inclusion and exclusion criteria were considered for

Mayo Clin Proc Inn Qual Out ■ June 2022;6(3):177-185 ■ https://doi.org/10.1016/j.mayocpiqo.2022.02.004
www.mcpiqojournal.org

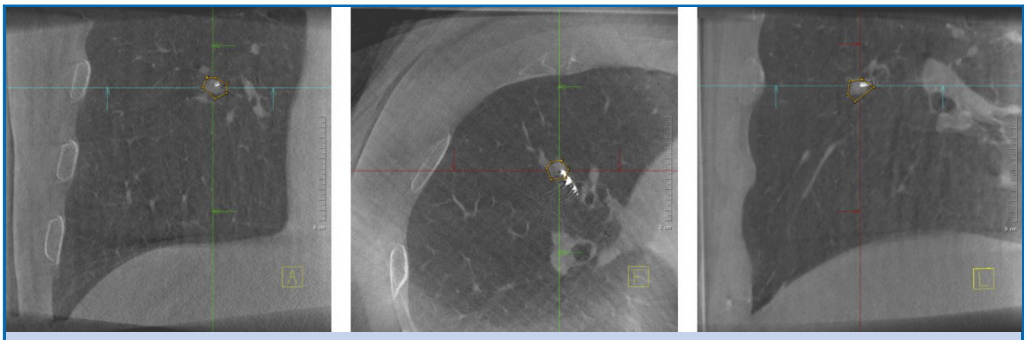

FIGURE 2. Intraprocedural cone-beam computed tomography scan with measurements in 3 axes demonstrating tool-in-lesion.

this study. CT scans were performed with the use of a standardized protocol with a slice thickness of 0.75-1 mm. All study procedures were performed with general anesthesia and neuromuscular blockade in a dedicated bronchoscopy suite.

Demographic data and nodule characteristics were recorded. Diagnostic yield was defined as a pathologic result that prompted a definitive treatment plan based on the Tumor Board review of the clinical case.

Procedure Description

Airway inspection and mucociliary clearance were performed with flexible bronchoscopy under general anesthesia with neuromuscular blockade for all patients. Tidal volumes were set between 6 and 8 mL/kg of ideal body weight, with adequate minute ventilation ensured and a predisposition for higher tidal volumes and lower respiratory rates. Upper lobe and lower lobe nodules were typically placed at a positive end-expiratory pressure (PEEP) of 12 and 15 cm H_2O, respectively. If the airway diameter appeared narrowed during the navigation, PEEP was increased incrementally by 2 cm H_2O. These anesthesia parameters were chosen on the basis of concerns of atelectasis diminishing biopsy yield. When hemodynamic tolerance is of utmost importance for patient safety, a PEEP of 10-12 cm H_2O is recommended for upper lobe biopsies with even higher values for lower lobe biopsies, especially in obese patients (Katsis et al[22] used a ventilation protocol with a PEEP of 15 cm H_2O achieving a pneumothorax complication rate of 2.5%).[22-24]

Following airway inspection, the SSRAB system (Ion Endoluminal Robotic Bronchoscopy System, Intuitive) was docked to the existing endotracheal tube (Figure 1). The Ion PlanPoint Planning Station incorporated a recent preoperative CT scan to create a 3D segmented airway model, which aided navigation to the lesion. The rEBUS probe was introduced through the working channel of the system and exchanged for a biopsy tool if a satisfactory signal was present.

After an idle time of at least 5 s, a 30-s intraoperative 3D mobile scan was used to visualize the biopsy tool and its relationship with the target nodule with an inspiratory 20 cm H_20 breath hold. Measurements were obtained in all 3 axes, which included distance to the nodule and the catheter orientation (Figure 2). Readjustment and another spin were performed, if necessary, before obtaining biopsy samples, to confirm the catheter location. Rapid on-site cytology evaluation was available for intraoperative feedback. Standard mediastinal staging or other components of the bronchoscopy were then performed. A postprocedural chest x-ray or a final 3D mobile imaging spin evaluated for pneumothorax. The patients had a 30-day phone follow-up to assess delayed postprocedural complications.

Calculating Divergence

Following completion of the procedure, CT images were imported to a digital imaging and communications in medicine viewer. The center of the lesion was identified in all 3 axes and assigned x, y, and z coordinates with respect to the orientation

TABLE 1. Patient, Nodule, and Procedure Characteristics[a]

Characteristic	Value
Patient	
Total no.	30
Male (%)	17 (56.7%)
Age (y), mean (range)	69.3 (35-87)
BMI (kg/m^2), mean (SD)	27.7 (6.14)
Smoking status	
Current (%)	5 (16.7%)
Former (%)	16 (53.3%)
Never smoker (%)	9 (30.0%)
Cancer history	
Lung	5
Breast	1
Colon	1
Hematologic	4
Genitourinary cancer	6
Other	7
Prior thoracic surgery	
Lobectomy	1
Wedge resection	2
Nodule size (mm)[b], median (SD),	17.5 (6.8)
10	3 (10.0%)
11-20	15 (50.0%)
21-29	9 (30.0%)
30	3 (10.0%)
Bronchus sign (%)	
Present	12 (40.0%)
Absent	18 (60.0%)
Nodule type	
Solid	23 (76.7%)
Semisolid	6 (20.0%)
Cavitary	1 (3.3%)
Nodule location (%)	
Right upper lobe	9 (30.0%)
Left upper lobe	9 (30.0%)
Right middle lobe	2 (6.7%)
Right lower lobe	7 (23.3%)
Left lower lobe	3 (10.0%)
Mean airway generation, number (SD)	7 (1.4)
Mean distance to pleura (mm), (SD)	14.9 (11.8)
Distance from nearest critical blood vessel, <5 mm	6 (20.0%)
Catheter adjustments	2.43
Number of spins, mean (SD)	2.5 (1.6)
Dose area product (Gy cm^2), mean (SD),	50.30 (32.0)
Total procedure time (min), mean (SD)	55.4 (35.1)
rEBUS signal	
Eccentric	19 (63.3%)
Concentric	4 (13.3%)
No view	7 (23.3%)

[a]BMI, body mass index; CT, computed tomography; rEBUS, radial endobronchial ultrasound.
[b]Measured as the largest diameter on CT imaging.

and position of the shape-sensing catheter when navigated to the virtual target. The position of the shape-sensing catheter was similarly recorded in the x, y, and z coordinates when the tool-in-lesion was obtained on the basis of mobile 3D imaging. These calculations generated 2 data points: catheter position on the basis of navigation to the virtual target from the preprocedural CT and catheter position on the basis of tool-in-lesion during real-time mobile CT imaging. Divergence was measured by calculating the displacement of the target from the preprocedure CT and intraoperative CBCT (Supplemental Figure, available online at http://www.mcpiqojournal.org).

End Points

The primary efficacy end point of this study was the ability to demonstrate navigation feasibility, which is defined as the ability to reach the preplanned target location and visualize the catheter tip oriented toward the lesion in 3 axes with the confirmation of "tool-in-lesion." Additional outcomes included the overall incidence of procedure-related complications, procedure-duration-related outcomes, divergence data, diagnostic yield, and radiation dose.

RESULTS

Demographic Details

Between February and August 2021, 30 nodules were sampled in 17 men (56.6%) and 13 women (43.3%) with a moderate-to-high probability of primary or secondary pulmonary malignancy (Table 1). Most patients had a clinically significant smoking history, with 16.7% still smoking at the time of the procedure. Seventeen patients had a documented history of chronic obstructive pulmonary disease or evidence of emphysema on imaging. Eighty-nine percent of patients with pulmonary function testing available for review had an ratio of force expiratory volume in one second to forced vital capcity less than 80%. Eighteen (60%) patients had a previous history of malignancy, with 5 patients having a history of lung cancer (4 patients had more than one type of malignancy).

Mayo Clin Proc Inn Qual Out ■ June 2022;6(3):177-185 ■ https://doi.org/10.1016/j.mayocpiqo.2022.02.004
www.mcpiqojournal.org

TABLE 2. Cases of Divergence[a]	
Target lesion from preprocedural and intraoperative CT with less than 10% overlap or less[b]	
Upper lobes (17)	Lower lobes (11)
Average lesion size: 16.5 mm	Average lesion size: 16.8 mm
Median divergence: 10 mm	Median divergence: 21 mm
Cases with divergence, 6 (35%) Average lesion size: 18.5 mm Median divergence: 17.8 mm	Cases with divergence, 8 (73%) Average lesion size: 14.2 mm Median divergence: 21.5 mm
Target centers from preprocedural CT and intraoperative 3D images divergent >10 mm[c]	
Upper lobes (17)	Lower lobes (11)
Average lesion size: 16.5 mm	Average lesion size: 16.8 mm
Median divergence: 10 mm	Median divergence: 21 mm
Cases with divergence, 8 (47%) Average lesion size: 15.3 mm Median divergence: 17 mm	Cases with divergence, 9 (82%) Average lesion size: 17 mm Median divergence: 22 mm

[a]CT, computed tomography.
[b]A total of 28 cases with 50% of cases demonstrating divergence.
[c]A total of 28 cases with 60% of cases demonstrating divergence.

Target Nodule Characteristics

Most of these nodules were located in the upper lobes (60%) with a median size of 17.5 mm (SD, 6.8) in the largest dimension. The mean airway generation was 7, with a mean distance to pleura of 14.9 mm (range, 1-45.8 mm). Bronchus sign was present in 40% of patients. Most (76.7%) of the nodules were solid (Table 1).

Procedure Characteristics

In 100% of procedures, the proceduralist was able to navigate to the lesion (Table 1). Nineteen (63.3%) cases had an eccentric rEBUS signal, 13.3% had a concentric signal, and 23.3% had no signal with rEBUS. The total mean fluoroscopy time was 8.7 min (range, 2-27 min). The total mean DAP was 50.3 Gy cm^2 with an average of 2.5 spins overall for all cases. There was an average of one additional spin after adjustments were made from initial navigation (range, 1-8). In 12 cases, a final spin was performed at the completion of the procedure to confirm the absence of pneumothorax. The total mean procedural time from robotic docking to the removal of the catheter was 55.4 min (range, 14-122 min). This time included rapid on-site cytology evaluation analysis and one instance of equipment malfunction in which forward progression of the catheter occurred and the system had to be rebooted.

Complications

There were no episodes of bleeding (defined as a prolonged wedge or therapeutic maneuvers such as iced saline) or episodes of pneumothorax immediately after operation or at 30 days after the procedure. Two patients could not complete the procedure because of hemodynamic instability (arrhythmia and hypotension), which could have been related to higher PEEP or tidal volume or anesthetic drugs chosen for the procedure. Both had procedures terminated before the biopsy attempt. Therefore, these patients were excluded from the analysis and deemed as withdrawn from the study. No further data were obtained on these patients. This would account for a complication rate of 6.25% of patients.

One patient died 4 months after the procedure (but during the study period) from complications of metastatic cancer, which were unrelated to the procedure.

Divergence

Divergence was defined as an overlap greater than 10% between the target location on the preprocedural CT and the target location during real-time mobile 3D imaging. On the basis of the definition of a 10% overlap between targets, divergence was identified in 50% of nodules, which in fact, increased to 60% when redefined on the basis of a distance of 10 mm between targets. Notably, this distinction

TABLE 3. Results of Biopsy and Diagnostic Yield On the Basis of Nodule Characteristics[a]

Malignancy	N	Infection	N	Inflammation	N
Squamous cell	4	Chronic necrotizing aspergillosis	1	Organizing pneumonia	2
Metastatic leiomyosarcoma	1			Granuloma	2
Metastatic adenocarcinoma, not primary lung	2			Focal interstitial fibrosis	1
Carcinoid	1				
Adenocarcinoma, lung primary	8				
Non-small-cell	4				
Small-cell	2				
Total	22 (73.3)	Total	1 (3.6)	Total	5 (17.9)
					Diagnostic yield[b]
Location					
Right upper lobe					8/9 (88.9%)
Left upper lobe					9/9 (100%)
Right middle lobe					2/2 (100%)
Right lower lobe					6/7 (85.7%)
Left lower lobe					3/3 (100%)
Bronchus sign present					12/12 (100%)
Bronchus sign absent					16/18 (88.9%)
rEBUS view					
Eccentric					18/19 (94.7%)
Concentric					4/4 (100%)
No view					6/7 (85.7%)
Lesion appearance					
Solid					22/23 (95.6%)
Semisolid					6/6 (100.0%)
Cavitary					0/1 (0%)
Size					
10 mm					3/3 (100%)
11-20 mm					13/15 (86.7%)
21-29 mm					9/9 (100%)
30 mm					3/3 (100%)

[a]rEBUS' radial endobronchial ultrasound.
[b]Defined as pathology correlating to treatment recommendations of Tumor Board.

was even more apparent when analyzed by location, where the median divergence ranged from 10 mm in the upper lobes to 21 mm in the lower lobes (Table 2).

Biopsy Results/Diagnostic Yield

Twenty-two patients had a diagnosis of malignancy confirmed on final pathology. Benign-specific pathology was identified in 6 patients (20.0%). Inconclusive pathology was obtained in 2 patients (Table 3). On the basis of our definition, this study yielded a diagnostic yield of 93.3% (Table 3). Our true positive rate was 73.3% (22/30 cases) with a 6.7% false-negative rate (2/30 cases), with an overall sensitivity for malignancy of 91.7%.

One patient's inconclusive biopsy result showed histiocytes; however, definitive treatment with stereotactic body radiation therapy was pursued on the basis of the probability that this was still a malignancy. The second patient with an inconclusive biopsy had a nondiagnostic CT-guided biopsy before the bronchoscopic procedure. The robotic biopsy was also nondiagnostic showing atypical cells, and the patient is still under observation.

Mayo Clin Proc Inn Qual Out ■ June 2022;6(3):177-185 ■ https://doi.org/10.1016/j.mayocpiqo.2022.02.004
www.mcpiqojournal.org

DISCUSSION

We have incorporated portable 3D imaging using the CIOS 3D Spin Mobile system into our workflow to confirm tool-in-lesion during our procedures as a complement to SSRAB. The robotic bronchoscope provides visual cues regarding the proximity of positioning and orientation to critical structures such as the pleura. The 3D mobile imaging spin then provides additional information on the spatial relationships between the catheter, airway, and nodule to enable position refinement through precise movement enabled by the robotic system, if needed, as well as capture tool-in-lesion, which is particularly important in distinguishing sampling errors from a true negative in the case of a benign nodule biopsy. In addition, the small footprint of the SSRAB along with the ability of the CIOS to be positioned around the patient facilitates its use in any room and appears to have a low radiation profile with no effect on the proceduralist's or anesthesiologist's workspace.[18]

Diagnostic yield for peripheral lesions via flexible bronchoscopy has been reported to be as low as 14% for peripheral nodules under 2 cm because of the difficulty in identifying the distance and the correct bronchus pathway.[8] In 2019, the results of the NAVIGATE trial, a large, multicenter, prospective cohort study, showed a diagnostic yield of 73% using ENB in 1215 patients.[10] In a randomized trial by Eberhardt et al,[25] the diagnostic yield was considerably higher with the combination of ENB and rEBUS (87.5%) than with ENB alone (59.0%). However, in a nonrandomized study, the diagnostic yield was 71.4% without rEBUS and 73.1% with rEBUS.[26] A subsequent meta-analysis showed a pooled (from 7872 lesions) diagnostic yield of 70.6%.[11] As recently reported, the use of SSRAB had a success navigation rate of 98.7% with an overall diagnostic yield of 81.7%.[27]

Despite the ability to detect an rEBUS signal, for small lesions even a slight movement may mean that the biopsy instrument misses the lesion entirely.[28] This may be due to unrecognized manual manipulation of the bronchoscope or from deflections during the insertion of the biopsy tool. Additionally, there is a known association between increased procedural time and atelectasis obscuring the results of localization.[29] The Ion robotic platform has been shown to successfully localize the target lesion in 96% of the cases and has an overall diagnostic yield of 79% with no pneumothorax or major bleeding complications.[13] In a more recent publication reporting 67 nodules, no pneumothorax or airway bleeding of any grade was reported.[30] In a larger cohort, the safety profile was reproduced with a 3.3% pneumothorax rate.[31]

To overcome the diaphragmatic movement affecting the nodule location and CT-to-body divergence, others have recommended the use of CBCT with great success.[32] In the NAVIGATE study, 4.9% of cases used CBCT for confirmation.[10] Robotic bronchoscopy was combined with CBCT and demonstrated increased sensitivity (84% procedural sensitivity for malignancy) and diagnostic accuracy (overall 86%) of lung nodules biopsied.[33] However, access to the rooms is limited and can lead to delays in scheduling and additional expenses.

The CIOS system has been described previously in limited case series. Avasarala et al[34] used this technology in conjunction with the superDimension Navigation System. Tool-in-lesion was obtained in 100% of procedures, but this did not correlate with diagnostic yield. Kalchiem-Dekel et al[14] also recently reported their experience with 10 lesions in 5 patients using the Intuitive Ion platform in conjunction with the CIOS Mobile 3D spin. They identified tool-in-lesion in 90% of their patients. The relationship between the biopsy tool and lesion was improved in 3 instances (30% of the time) after the subsequent redeployment of the tool, which was based on direct feedback from the intraoperative portable CT imaging.[14] The result of our study is in agreement with these results, with an overall tool-in-lesion rate of 97%, with an average of only 1 manipulation per nodule.

Radiation dose is an important metric that is captured during interventional procedures. A previous pilot study had shown that CBCT-guided bronchoscopy is associated with acceptable radiation dose and potentially increases diagnostic yield.[18] Given that the CIOS gives a predominantly fluoroscopic

image, radiation is measured as the DAP or the kerma area product. DAP is defined as a product of dose and beam area (Gy cm^2) and is measured using an ionization chamber placed between the x-ray tube/collimator setup and the patient.[35] A recent study describing the use of mobile 3D imaging in a small subset of patients showed an average dose of 40.9253 Gy cm^2 with 8.4 min of fluoroscopy time.[34] This is to be compared with a mean DAP of 64.57 Gy cm^2 for a total fluoroscopy time of 8.6 min measured by fixed CBCT (Siemens Artis dTA angiography system) manufactured by the same company.[18] Subsequent papers have reported an initial radiation dose of 47.5 Gy cm^2, which decreased to 25.4 Gy cm^2 with additional experience.[20] For comparison, a standard chest CT requires a DAP of 40-60 Gy cm^2.[36] Our study showed an average of 8.7 min of fluoroscopy time and a DAP of 50.3 Gy cm^2 ($\pm$32.0 Gy cm^2), corroborating earlier studies that the initial radiation dosage for these types of procedures is similar. Like the previous study, with increased patient volumes improving the learning curve, this dosage can likely be decreased over time.

Although previous studies have shown that the divergence phenomenon exists, little data is present to demonstrate a reproducible mechanism to quantitatively calculate divergence. Pritchett et al[16] described the phenomenon and related it to multiple patient and procedural factors. Chen et al[37] reported a divergence of up to 17 mm when assessing the change between CTs at full expiration and full inhalation. This is the first publication, to our knowledge, to develop an algorithm to calculate intraprocedural divergence and demonstrate that subtle changes in nodule motion can occur in up to 50%-60% of patients. The authors conclude that, on the basis of the reported diagnostic yield of this study, with a combination of a reliable navigation tool, imaging system, and appropriate ventilatory parameters and strategies, divergence can be overcome to successfully biopsy indeterminate pulmonary nodules.

This study has several limitations. Despite being a prospective study, the sample size is small. In addition, although patients were excluded if the probability of malignancy was low, this may have been attributed to an element of unconscious selection bias. Although the patients were encouraged to seek alternate methods of biopsy if the diagnosis was unclear, the 2 patients were ultimately elected for observation, which did make their ultimate diagnosis somewhat presumptive. Finally, this is the first publication to attempt the calculation of divergence with a preliminary analysis, thus needing further validation in a larger cohort.

CONCLUSION

In conclusion, the combination of mobile 3D imaging and shape-sensing robotic bronchoscopic biopsy of pulmonary nodules shows early promise to achieve acceptable diagnostic yield and radiation dose to overcome nodule motion and divergence in most patients.

AUTHOR CONTRIBUTIONS

Dr Reisenauer contributed substantially to the study design, data interpretation, and writing of the manuscript. Dr Duke contributed substantially to data analysis and interpretation and writing of the manuscript. Drs Reisenauer and Duke had full access to all the data in the study and take responsibility for the integrity of the data and the accuracy of the data analysis, including and especially any adverse effects. Drs Kern, Fernandez-Bussy, and Edell recruited patients and assisted with manuscript writing and data interpretation.

SUPPLEMENTAL ONLINE MATERIAL

Supplemental material can be found online at http://www.mcpiqojournal.org. Supplemental material attached to journal articles has not been edited, and the authors take responsibility for the accuracy of all data.

Abbreviations and Acronyms: **3D**, three dimensional; **CBCT**, cone-beam computed tomography; **CT**, computed tomography; **DAP**, dose area product; **ENB**, electromagnetic navigation; **PEEP**, positive end-expiratory pressure; **rEBUS**, radial endobronchial ultrasound; **SSRAB**, shape-sensing robotic-assisted bronchoscopy

All datasets are readily available to editors, reviewers, and readers without unnecessary restriction wherever possible.

Grant Support: Siemens provided the equipment in kind/funding provided by the Simons Family Career Benefactor award. The authors received no financial support for the research, authorship, and/or publication of this article.

Potential Competing Interest: Dr Reisenauer has an independent research grant with Intuitive Surgical Inc. The other authors report no competing interests.

Correspondence: Address to Janani Reisenauer, MD, Division of General Thoracic Surgery, Mayo Clinic, 200 1st St, SW, Rochester, MN 55905 (reisenauer.janani@mayo.edu).

REFERENCES

1. Ferlay J, Colombet M, Soerjomataram I, et al. Estimating the global cancer incidence and mortality in 2018: GLOBOCAN sources and methods. *Int J Cancer*. 2019;144(8):1941-1953.
2. Siegel RL, Miller KD, Jemal A. Cancer statistics, 2018. *CA Cancer J Clin*. 2018;68(1):7-30.
3. Prevention CfDCa. *An Update on Cancer Deaths in the United States*. Atlanta, GA: Department of Health and Human Services, Centers for Disease Control and Prevention, Division of Cancer Prevention and Control; 2021.
4. Lu T, Yang X, Huang Y, et al. Trends in the incidence, treatment, and survival of patients with lung cancer in the last four decades. *Cancer Manag Res*. 2019;11:943-953.
5. Spiro SG, Gould MK, Colice GL, et al. Initial evaluation of the patient with lung cancer: symptoms, signs, laboratory tests, and paraneoplastic syndromes: ACCP evidenced-based clinical practice guidelines (2nd edition). *Chest*. 2007;132(3 suppl):149S-160S.
6. Institue NC. Cancer Stat Facts: Lung and Bronchus Cancer: NIH; 2021. https://seer.cancer.gov/statfacts/html/lungb.html. Accessed October 30, 2021.
7. Force USPST, Krist AH, Davidson KW, et al. Screening for lung cancer: US preventive services task force recommendation statement. *JAMA*. 2021;325(10):962-970.
8. Baaklini WA, Reinoso MA, Gorin AB, et al. Diagnostic yield of fiberoptic bronchoscopy in evaluating solitary pulmonary nodules. *Chest*. 2000;117(4):1049-1054.
9. Hiraki T, Mimura H, Gobara H, et al. Incidence of and risk factors for pneumothorax and chest tube placement after CT fluoroscopy-guided percutaneous lung biopsy: retrospective analysis of the procedures conducted over a 9-year period. *AJR Am J Roentgenol*. 2010;194(3):809-814.
10. Folch EE, Pritchett MA, Nead MA, et al. Electromagnetic navigation bronchoscopy for peripheral pulmonary lesions: one-year results of the prospective, multicenter NAVIGATE study. *J Thorac Oncol*. 2019;14(3):445-458.
11. Ali MS, Sethi J, Taneja A, et al. Computed tomography bronchus sign and the diagnostic yield of guided bronchoscopy for peripheral pulmonary lesions. a systematic review and meta-analysis. *Ann Am Thorac Soc*. 2018;15(8):978-987.
12. Chaddha U, Kovacs SP, Manley C, et al. Robot-assisted bronchoscopy for pulmonary lesion diagnosis: results from the initial multicenter experience. *BMC Pulm Med*. 2019;19(1):243.
13. Fielding DIK, Bashirzadeh F, Son JH, et al. First human use of a new robotic-assisted fiber optic sensing navigation system for small peripheral pulmonary nodules. *Respiration*. 2019;98(2):142-150.
14. Kalchiem-Dekel O, Fuentes P, Bott MJ, et al. Multiplanar 3D fluoroscopy redefines tool-lesion relationship during robotic-assisted bronchoscopy. *Respirology*. 2021;26(1):120-123.
15. Chen AC, Pastis NJ Jr, Mahajan AK, et al. Robotic bronchoscopy for peripheral pulmonary lesions: a multicenter pilot and feasibility study (BENEFIT). *Chest*. 2021;159(2):845-852.
16. Pritchett MA, Bhadra K, Calcutt M, et al. Virtual or reality: divergence between preprocedural computed tomography scans and lung anatomy during guided bronchoscopy. *J Thorac Dis*. 2020;12(4):1595-1611.
17. Cheng GZ, Liu L, Nobari M, et al. Cone beam navigation bronchoscopy: the next frontier. *J Thorac Dis*. 2020;12(6):3272-3278.
18. Casal RF, Sarkiss M, Jones AK, et al. Cone beam computed tomography-guided thin/ultrathin bronchoscopy for diagnosis of peripheral lung nodules: a prospective pilot study. *J Thorac Dis*. 2018;10(12):6950-6959.
19. Abi-Jaoudeh N, Fisher T, Jacobus J, et al. Prospective randomized trial for image-guided biopsy using cone-beam CT navigation compared with conventional CT. *J Vasc Interv Radiol*. 2016;27(9):1342-1349.
20. Verhoeven RLJ, van der Sterren W, Kong W, et al. Cone-beam CT and augmented fluoroscopy-guided navigation bronchoscopy: radiation exposure and diagnostic accuracy learning curves. *J Bronchology Interv Pulmonol*. 2021;28(4):262-271.
21. Verhoeven RLJ, Futterer JJ, Hoefsloot W, et al. Cone-beam CT image guidance with and without electromagnetic navigation bronchoscopy for biopsy of peripheral pulmonary lesions. *J Bronchology Interv Pulmonol*. 2021;28(1):60-69.
22. Katsis J, Roller L, Aboudara M, et al. Diagnostic yield of digital tomosynthesis-assisted navigational bronchoscopy for indeterminate lung nodules. *J Bronchology Interv Pulmonol*. 2021;28(4):255-261.
23. Bhadra K, Setser RM, Condra W, et al. Lung navigation ventilation protocol to optimize biopsy of peripheral lung lesions. *J Bronchology Interv Pulmonol*. 2022;29(1):7-17.
24. Pritchett MA, Lau K, Skibo S, et al. Anesthesia considerations to reduce motion and atelectasis during advanced guided bronchoscopy. *BMC Pulm Med*. 2021;21(1):240.
25. Eberhardt R, Anantham D, Ernst A, et al. Multimodality bronchoscopic diagnosis of peripheral lung lesions: a randomized controlled trial. *Am J Respir Crit Care Med*. 2007;176(1):36-41.
26. Ozgul G, Cetinkaya E, Ozgul MA, et al. Efficacy and safety of electromagnetic navigation bronchoscopy with or without radial endobronchial ultrasound for peripheral lung lesions. *Endosc Ultrasound*. 2016;5(3):189-195.
27. Kalchiem-Dekel O, Connolly JG, Lin IH, et al. Shape-sensing robotic-assisted bronchoscopy in the diagnosis of pulmonary parenchymal lesions. *Chest*. 2022;161(2):572-582.
28. Ashraf SF, Lau KKW. Navigation bronchoscopy: a new tool for pulmonary infections. *Med Mycol*. 2019;57(suppl 3):S287-S293.
29. Sagar AS, Sabath BF, Eapen GA, et al. Incidence and location of atelectasis developed during bronchoscopy under general anesthesia: the I-LOCATE trial. *Chest*. 2020;158(6):2658-2666.
30. Simoff MJ, Pritchett MA, Reisenauer JS, et al. Shape-sensing robotic-assisted bronchoscopy for pulmonary nodules: initial multicenter experience using the ion endoluminal system. *BMC Pulm Med*. 2021;21(1):322.
31. Reisenauer J, Simoff MJ, Pritchett MA, et al. Ion: technology and techniques for shape-sensing robotic-assisted bronchoscopy. *Ann Thorac Surg*. 2022;113(1):308-315.
32. Pritchett MA, Schampaert S, de Groot JAH, et al. Cone-beam CT with augmented fluoroscopy combined with electromagnetic navigation bronchoscopy for biopsy of pulmonary nodules. *J Bronchology Interv Pulmonol*. 2018;25(4):274-282.
33. Benn BS, Romero AO, Lum M, et al. Robotic-assisted navigation bronchoscopy as a paradigm shift in peripheral lung access. *Lung*. 2021;199(2):177-186.
34. Avasarala SK, Machuzak MS, Gildea TR. Multidimensional precision: hybrid mobile 2D/3D C-arm assisted biopsy of peripheral lung nodules. *J Bronchology Interv Pulmonol*. 2020;27(2):153-155.
35. Bushberg JT. *The Essential Physics of Medical Imaging*. 3rd ed. Wolters Kluwer Health/Lippincott Williams & Wilkins; 2012; xii:1030.
36. Nickoloff EL, Lu ZF, Dutta AK, et al. Radiation dose descriptors: BERT, COD, DAP, and other strange creatures. *Radiographics*. 2008;28(5):1439-1450.
37. Chen A, Pastis N, Furukawa B, et al. The effect of respiratory motion on pulmonary nodule location during electromagnetic navigation bronchoscopy. *Chest*. 2015;147(5):1275-1281.